Annu. Rev. Fluid Mech. 2010.42:43-66. Downloaded from www.annualreviews.org
by University of California - Berkeley on 02/08/12. For personal use only.

ANNUAL REVIEWS Further
Click here for quick links to Annual Reviews content online, including:
• Other articles in this volume
• Top cited articles
• Top downloaded articles
• Our comprehensive search

Fluvial Sedimentary Patterns

G. Seminara

Department of Civil, Environmental, and Architectural Engineering, University of Genova, 16145 Genova, Italy; email: sem@diam.unige.it

Annu. Rev. Fluid Mech. 2010. 42:43–66

First published online as a Review in Advance on August 17, 2009

The *Annual Review of Fluid Mechanics* is online at fluid.annualreviews.org

This article's doi:
10.1146/annurev-fluid-121108-145612

Copyright © 2010 by Annual Reviews.
All rights reserved

0066-4189/10/0115-0043$20.00

Key Words

sediment transport, morphodynamics, stability, meander, dunes, bars

Abstract

Geomorphology is concerned with the shaping of Earth's surface. A major contributing mechanism is the interaction of natural fluids with the erodible surface of Earth, which is ultimately responsible for the variety of sedimentary patterns observed in rivers, estuaries, coasts, deserts, and the deep submarine environment. This review focuses on fluvial patterns, both free and forced. Free patterns arise spontaneously from instabilities of the liquid-solid interface in the form of interfacial waves affecting either bed elevation or channel alignment: Their peculiar feature is that they express instabilities of the boundary itself rather than flow instabilities capable of destabilizing the boundary. Forced patterns arise from external hydrologic forcing affecting the boundary conditions of the system. After reviewing the formulation of the problem of morphodynamics, which turns out to have the nature of a free boundary problem, I discuss systematically the hierarchy of patterns observed in river basins at different scales.

1. PHENOMENOLOGICAL INTRODUCTION

Transport capacity: rate at which a stream is capable of carrying sediment under equilibrium conditions (no net erosion nor net deposition)

Let us start our journey with a broad, phenomenological introduction to sedimentary patterns. They are the expressions of the interaction between flowing fluids and the erodible surface of Earth. Seeking to be somewhat systematic, one may use various paradigms to organize field observations while wandering through fluvial environments.

First, a fundamental distinction may be made among erosional, depositional, and equilibrium patterns: The rate at which sediment is supplied to the system is respectively smaller than, larger than, or equal to the rate at which the system is capable of transporting it. Erosional patterns develop typically in the upper parts of river basins where sediment is produced. Hillslopes (**Figure 1*a***) and meanders in rocks are just two examples. Depositional patterns occur at the foot of mountains or hillslope incisions (subaerial alluvial fans) and at river mouths (fluvial deltas) (**Figure 1*b***): In the depositional case, the ultimate mechanism of pattern formation is a break in flow velocity, hence in the transport capacity of the stream. Bed forms, under steady forcing (e.g., fluvial ripples, dunes, and bars), are examples of equilibrium patterns.

A second important paradigm is the distinction between free and forced patterns. The former ones arise spontaneously, from the instability of the liquid-solid interface in the form of interfacial waves affecting the boundary: Bed forms and river planforms are most often expressions of a free response. On the contrary, erosional and depositional patterns are forced by hydrologic factors at the boundary of the fluvial reach.

A third major paradigm involves the key concept of spatial and temporal scales. Patterns can be classified as small-, meso-, or large-scale depending on their typical wavelengths, scaling with flow depth, channel width, or some larger scale. Patterns of different spatial (and temporal) scales may coexist but usually require distinct theoretical tools for investigation, in particular, distinct spatially and temporally averaged descriptions of sediment transport.

Finally, patterns may be recognized in various characteristics of the channel boundary. The instability of the bed interface affects bed elevation (bed forms). Similarly, the straight alignment of fluvial channels is typically unstable to planform perturbations arising from a complex interaction between outer-bank erosion (a mechanism whereby the floodplain loses sediment to the channel) and inner-bank deposition (a mechanism of floodplain reconstruction). As a result, planform patterns develop, either building up channel sinuosity (meandering) (**Figure 2*a***) or

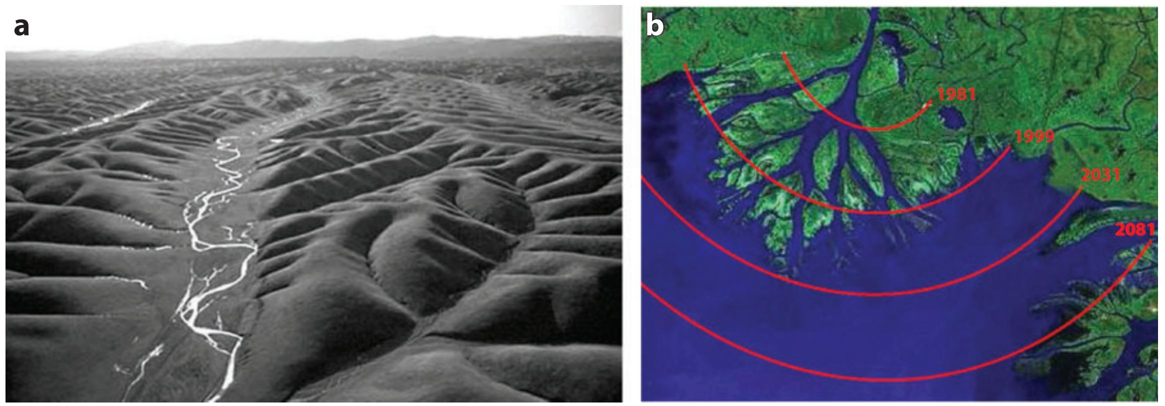

Figure 1

(*a*) Erosional pattern: landscape near Orland, California, with rhythmic sequences of valleys spaced roughly 100 m apart. Figure courtesy of J. Kirchner. (*b*) Depositional pattern: the Wax Lake fluvial delta, Louisiana. Red lines show predictions (Parker & Sequeiros 2006) of its progradation in time. Figure courtesy of G. Parker.

Annu. Rev. Fluid Mech. 2010.42:43-66. Downloaded from www.annualreviews.org
by University of California - Berkeley on 02/08/12. For personal use only.

Annu. Rev. Fluid Mech. 2010.42:43-66. Downloaded from www.annualreviews.org
by University of California - Berkeley on 02/08/12. For personal use only.

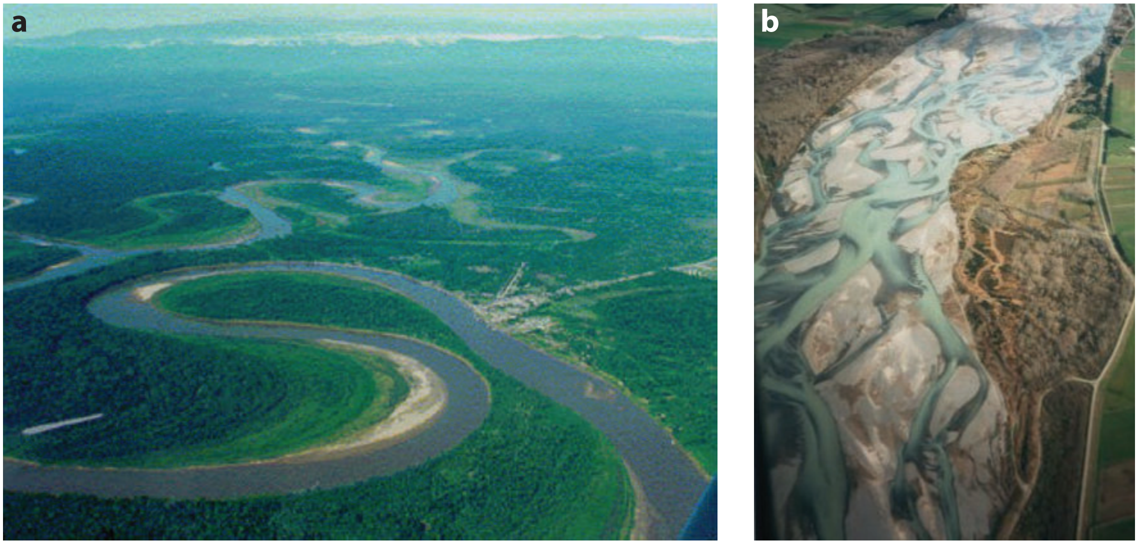

Figure 2

(*a*) Forced (steady) bar at the inner bend of a meander very close to neck cutoff, a process occurring when two meander branches merge, cutting the meander loop. Historical bend development can be traced by the sequence of so-called scroll bars showing up in the flood plain adjacent to the inner bend. (*b*) Multiple row (migrating) bars in the Waikariri River, a braiding river of New Zealand (courtesy of B. Federici).

forming an interconnected network of curved channels (braiding) (**Figure 2*b***). Finally, so-called sorting patterns may be recognized in the spatial arrangement of the grain-size distribution of poorly sorted sediment mixtures: Their expression is the development of stationary or migrating rhythmic sequences of coarser and finer material (**Figure 3*b*,*c***).

Morphodynamics: a novel discipline concerned with the understanding of processes whereby sediment motion is able to shape Earth's surface

2. MORPHODYNAMICS: A FREE-BOUNDARY PROBLEM

We are concerned with the gravitationally driven motion of water bounded by a free surface and by an erodible medium. The flow, referring to a fixed Cartesian reference frame (x_1, x_2, x_3) with

TIDAL PATTERNS

Equally fascinating, sedimentary patterns are displayed in tidally dominated environments. In particular, lagoon networks originate from inlets where the channel bottom is typically composed of fine sediments (medium-fine sand). Proceeding landward, channel width, depth, and sediment size decrease, whereas the tide is allowed to expand into typically muddy and shallow regions (tidal flats) adjacent to the main and secondary channels. Lagoon patterns present analogies with fluvial patterns as well as distinct features. First, equilibrium is quasi-static rather than dynamic. Second, interface instability is of Floquet type because of the oscillatory character of tidal flow. Patterns are mostly symmetrical and hardly develop fronts. Deviations from symmetry as well as pattern migration are driven by residual currents and/or flood-ebb dominance of the basic state. Third, cohesion as well as bioturbation and wind turbulence play a major role in the process of sediment resuspension in mudflats. Fourth, a major interaction with ecology is needed to understand the equilibrium of salt marshes, sinks of sediment whose efficiency depends on the survival of halophytic vegetation, which in turn depends crucially on sea-level rise and sediment availability.

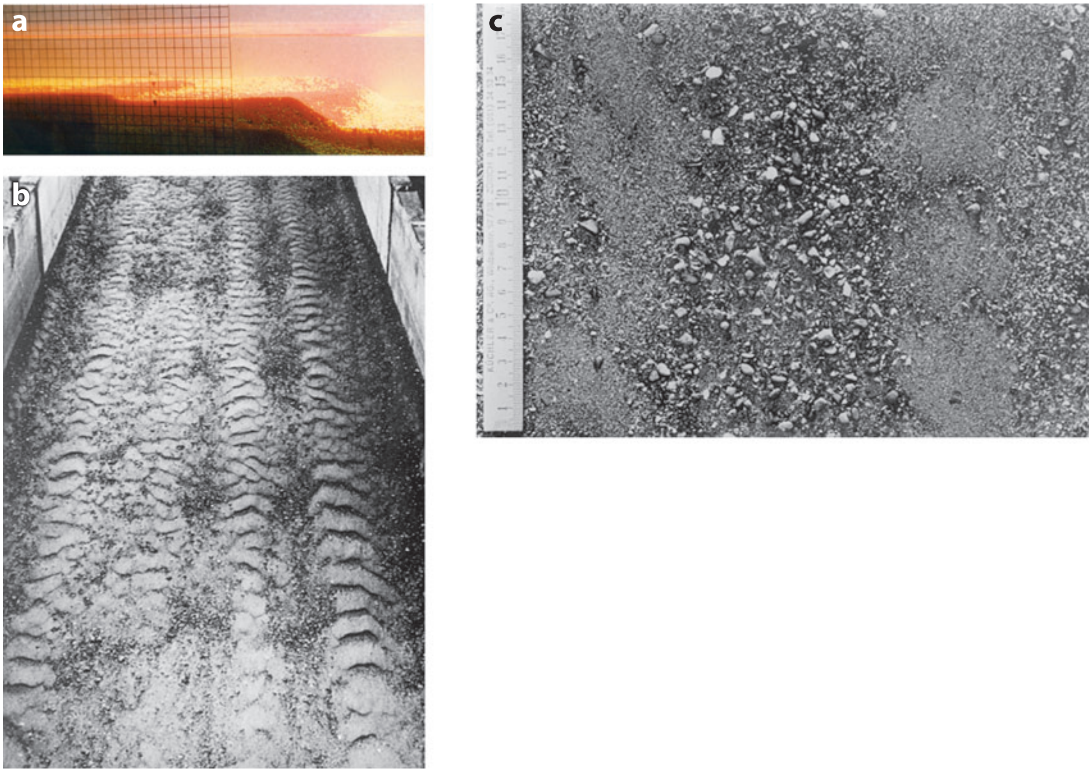

Figure 3

(a) Smaller dune migrating over the stoss side of a larger dune in bimodal sand mixtures (*red* is fine sand, and *yellow* is coarse). Figure courtesy of M. Colombini. (b) Longitudinal streaks are small-scale bed forms aligned with the channel axis. If sediment is heterogeneous, streaks cause a sorting mechanism whereby finer (coarser) material accumulates in the crests (troughs). This is clear in the panel, which shows ripples developed on the fine streaks. Flow is from bottom to top (Colombini & Parker 1995). Original photograph from Gunter 1971. (c) Close-up of the bed.

x_3 vertical coordinates pointing upward, is defined in the domain $\eta < x_3 < h$, where $\eta(x_1, x_2, t)$ and $h(x_1, x_2, t)$ are the elevations of the bed interface and of the free surface, respectively, and t is time. The erodible medium fills up the region $x_3 < \eta$.

2.1. Evolution Equation of the Bed Interface

The interface separating the fluid from the adjacent erodible medium is a free boundary allowing for the exchange of sediment particles between the two media: Particles are hydrodynamically entrained by the stream, are then advected by the flow, and settle back over the bed owing to their excess weight. As the near-bed concentration of the flowing mixture is much lower than the packing concentration c_M of the underlying granular medium, the stream loses (gains) sediments if the elevation of the bed interface increases (decreases). Allowing also for tectonic uplift $\mathcal{U}$ and subsidence $\mathcal{S}$, which play a role in patterns characterized by sufficiently large temporal scale, the following statement of the mass conservation of the solid phase must be satisfied:

$$c_M \eta_{,t} + \mathcal{E} - \mathcal{D} = \mathcal{U} - \mathcal{S}, \qquad (1)$$

Annu. Rev. Fluid Mech. 2010.42:43-66. Downloaded from www.annualreviews.org
by University of California - Berkeley on 02/08/12. For personal use only.

where $\mathcal{E}(\mathcal{D})$ is the entrained (deposited) sediment flux, namely the rate at which the volume of sediments per unit horizontal area is entrained from (deposited on) the bed. A sedimentary environment is erosional (depositional) if $\mathcal{E} > \mathcal{D}$ ($\mathcal{E} < \mathcal{D}$), whereas morphological equilibrium implies $\mathcal{E} = \mathcal{D}$. Needless to say, equilibrium may have to be understood in some (spatially or temporally) averaged sense. Simple continuity arguments allow the expression of the rate of aggradation (degradation) experienced by the bed ($\mathcal{E} - \mathcal{D}$) in terms of the sum of the rate of change of the average sediment content of the water column plus the horizontal divergence ($\boldsymbol{\nabla}_h \cdot$) of the depth-integrated sediment flux per unit width averaged over turbulence $\mathbf{q}_s$. Denoting by $\mathcal{C}$ the depth-averaged sediment concentration, the fundamental equation of morphodynamics takes the form

Entrainment: process whereby a fluid, moving over a cohesionless or cohesive granular medium, is able to detach particles from the boundary

$$c_M \eta_{,t} + (D\mathcal{C})_{,t} + \nabla_h \cdot \mathbf{q_s} = \mathcal{U} - \mathcal{S}, \tag{2}$$

where D is the local and instantaneous flow depth. This is a generalized version of the classical Exner equation (Exner 1925), which is obtained from Equation 2 by setting $\mathcal{U} = \mathcal{S} = 0$. Progress with Equation 2 requires the evaluation of $\mathbf{q}_s$ and $\mathcal{C}$. Rigorous theoretical predictions of these quantities would require numerical simulations of particle entrainment, transport, and deposition in a high–Reynolds number rough turbulent shear flow, an effort still beyond present theoretical and computational capabilities despite recent promising attempts (Schmeeckle & Nelson 2003). Progress in understanding morphodynamics, however, has been achieved on the basis of experimental observations. Some elementary knowledge required to follow the present review is summarized below.

Annu. Rev. Fluid Mech. 2010.42:43-66. Downloaded from www.annualreviews.org
by University of California - Berkeley on 02/08/12. For personal use only.

2.2. Sediment Transport

The mechanical processes responsible for sediment transport vary in different parts of river basins. It is convenient to distinguish regions where transport is supply limited from those where the stream is typically able to express its whole capacity of conveying sediments.

The transport capacity of fluvial streams. Experimental observations suggest that a uniform free-surface flow over a cohesionless plane bed is unable to entrain sediments below a critical value τ_{*c} of the ratio between measures of hydrodynamic (destabilizing) and gravitational (stabilizing) forces acting on sediment particles, the so-called Shields stress τ_* (Shields 1936). This quantity reads $[u_*^2/(s-1)gd]$, where u_* is the friction velocity, s is the relative particle density, d is an effective particle diameter, and g is gravity. The value of τ_{*c} is a function of grain size through the particle Reynolds number R_p ($\equiv \sqrt{(s-1)gd^3}/\nu$), with ν as the kinematic viscosity. For values of τ_* exceeding τ_{*c}, particles are entrained, either individually or collectively, by the spatially and temporally intermittent generation of turbulent sweeps in the near-wall region (Drake et al. 1988).

Particles then move (mostly saltating) close to the bed forming a layer a few grain diameters thick, eventually coming to rest to be entrained again after some time. This is called bed-load transport, in which particles have a distinct dynamics driven by, but different from, the dynamics of fluid particles. Observations and saltation models suggest that, under equilibrium conditions, the intensity of the bed-load flux per unit width q_s is a monotonically increasing nonlinear function of the excess Shields stress $\Phi(\tau_* - \tau_{*c})$, typically expressed in the form of a power law. Alternatively, on the basis of physical observations, one may estimate the sediment pickup rate $\mathcal{E}$ in terms of the local value of the Shields stress and the sediment deposition rate $\mathcal{D}$ in terms of a distribution function f of the step length of saltating particles (Nakagawa & Tsujimoto 1980). Hence,

$$\mathcal{E} = \mathcal{E}(\tau_* - \tau_{*c}); \quad \mathcal{D} = \int_0^\infty \mathcal{E}[\tau_*(s) - \tau_{*c}]\, f(s;\Lambda)\, ds, \tag{3}$$

where s is the distance from the pickup point, and Λ is the mean value of the step length. At equilibrium (i.e., if τ_* is spatially constant), the latter expression reduces to the equality $\mathcal{E} = \mathcal{D}$.

The direction of bed-load flux is aligned with the direction of the local average bottom stress, provided the bed is horizontal. Bed-load transport on weakly sloping beds feels the effect of gravity in two respects: On the one hand, a positive (negative) longitudinal slope reduces (increases) the critical Shields stress (Lysne 1969); hence it enhances (reduces) the intensity of bed-load transport. On the other hand, a deviation of the direction of bed-load transport from the longitudinal direction is driven by the lateral slope (Parker 1984). With the help of the weak slope assumption, one finds

$$\mathbf{q}_s = \Phi(\tau_* - \tau_{*c})\left[\left(1 - \frac{r_x}{\tau_* - \tau_{*c}}\eta_{,x}\right)\hat{x} - \frac{r_y}{\sqrt{\tau_*}}\eta_{,y}\hat{\mathbf{y}}\right], \tag{4}$$

where $\hat{\mathbf{x}}$ and $\hat{\mathbf{y}}$ are horizontal unit vectors aligned with and orthogonal to the bottom stress, respectively, whereas r_x and r_y are empirical constants.

As the Shields stress exceeds a second threshold value τ_{*s}, again a function of grain size through the particle Reynolds number R_p, sufficiently intense ejection events allow particles to escape the near-wall logarithmic barrier. Provided particles are small enough and the suspension is sufficiently dilute, particles are then nearly passively advected by the stream (i.e., their dynamics is distinct from that of fluid particles only in their tendency to settle). This is called transport in suspension. Entrainment and deposition fluxes are then expressed in the form

$$\mathcal{E} = W_s c_e(\tau_*); \quad \mathcal{D} = W_s c|_\eta, \tag{5}$$

where W_s is the settling speed of sediment particles, $c|_\eta$ is the local value of near-bed concentration, and c_e is the value of near-bed concentration that would be experienced in a uniform flow characterized by the same value of bottom stress: Hence, the net flux exchanged by the stream with the granular medium is proportional to the excess near-bed concentration relative to its equilibrium value. The latter quantity is an empirically known monotonically increasing function of the local Shields stress. The value of $c|_\eta$ is obtained from the solution of an advection-diffusion equation for concentration, requiring closure assumptions for turbulent diffusion (see Garcia 2008 for a recent assessment of the state of the art).

For very large values of the Shields stress, suspensions become highly concentrated, and a distinct bed interface is no longer distinguishable: These extreme forms of sediment transport occur impulsively in hillslope incisions, where material accumulates for a variety of reasons (e.g., landslides or volcanic eruptions) and gives rise to so-called mudflows, debris flows, and lahars. Erosive and depositional patterns associated with these phenomena are excluded from the present overview.

Detachment-limited sediment transport. Landscape evolution is driven by the mass movement and detachment of material from the land's surface. In soil-mantled landscapes, the dominant form of mass movement is creep, caused by bioturbation, frost heaving, and wetting-drying cycles. The associated unit sediment flux $\mathbf{q}_{sm}$ can be related to the topographic gradient through a Fick law with morphological diffusivity D_m (Culling 1965). The transport rate in the channelized portion of the landscape is limited by the rate of detachment and sediment entrainment by the overland flow: In other words, transport is not at capacity, but rather is detachment-limited, such that no redeposition of eroded sediment occurs. The detachment-driven entrained flux $\mathcal{E}_d = \nabla \cdot \mathbf{q}_{sd}$ is modeled as proportional to the excess shear stress relative to a cohesive threshold τ_c (Howard 1994). Hence, the morphodynamics of landscape evolution is modeled assuming

$$\nabla \cdot \mathbf{q}_s = -D_m \nabla^2 \eta + k_d(\tau - \tau_c)(\tau > \tau_c). \tag{6}$$

Annu. Rev. Fluid Mech. 2010.42:43-66. Downloaded from www.annualreviews.org
by University of California - Berkeley on 02/08/12. For personal use only.

Sedimentary patterns ultimately arise from the evolution of the bed interface. Equation 2, along with the appropriate form of the hydrodynamic equations required to determine the fluid stress at the boundary, poses a free-boundary problem for the unknown pattern of the bed interface. It is then instructive to analyze some general properties of Equation 2.

2.3. Properties of the Free Boundary Problem

A first property arises from purely dimensional arguments. In fact, perturbations of bed elevation scale with flow depth D_0; an appropriate horizontal scale (e.g., l) is set by the geometry of the particular pattern investigated. The intensity of the sediment flux per unit width q_s may vary widely depending on the environment and hydrodynamic conditions: However, in fluvial as well as in tidal environments, the depth-averaged sediment concentration hardly attains values as large as 10^{-3}; hence the scale Q_{s0} is at most of the order of $(10^{-3}\ U_0 D_0)$, with U_0 scale for the depth-averaged flow velocity. It follows from Equation 2 that the bed interface evolves on a morphological timescale t_M of the order of (or larger than) $10^3 l/U_0$. This scale must be compared with the hydrodynamic response time t_H, namely the time required for surface waves to propagate over the horizontal scale l. Typically, long waves travel with speed $(F_0 \pm 1)\sqrt{gD_0}$, where F_0 is the local Froude number; hence t_M is at least a factor $10^3(1 \pm F_0^{-1})$ larger than t_H. Physically, this implies that, except for near critical streams ($F_0 \simeq 1$), the flow adjusts quasi-instantaneously to the evolution of the bed interface. In other words, provided flow perturbations are driven only by bed perturbations, morphodynamics may be decoupled from hydrodynamics. On the contrary, decoupling is not allowed close to criticality or whenever the flow field varies on an externally imposed timescale t_E comparable with t_M: The latter case is relevant to the morphodynamic response of fluvial streams to flood propagation.

A second important property of Equation 2 is that it allows for the growth and migration of interfacial waves that arise from instabilities of the bed interface itself rather than from flow instabilities that can destabilize the boundary. The basic mechanism underlying such instabilities can be illustrated considering small-amplitude perturbations of some steady, basic bed elevation η_0: These perturbations drive linear perturbations of the bottom stress, hence of the sediment flux, which may lag relative to bottom perturbations depending on a variety of hydrodynamic and sedimentological factors. Equation 2 constrains these perturbations to satisfy the dispersion relationship

$$\omega = \boldsymbol{\lambda} \cdot \mathbf{q}_\eta \exp(-i\phi), \tag{7}$$

where $\boldsymbol{\lambda}$ is a two-dimensional (2D) real wave-number vector, ω is complex frequency, $\mathbf{q}_\eta = \mathbf{q}_{s,\eta}|_{\eta_0}$ is the real amplitude of the perturbation of sediment flux driven by perturbations of bed elevation, and ϕ is its phase lag. Both $\mathbf{q}_\eta$ and ϕ are functions of the basic state and of the perturbation wave number; hence instability may arise, depending on the hydrodynamic and sedimentological conditions within a specific wave-number range. The above mechanism was originally proposed by Kennedy (1963) for the case of 2D fluvial dunes (Section 4).

A third related issue is that interfacial waves are essentially vectors of morphodynamic information; hence their migration speed determines the rate and direction of propagation of such information.

Fourth, a significant feature most often displayed by interfacial waves is a tendency toward wave peaking and the possible occurrence of fronts with slopes close to the angle of repose of the granular medium. Depositional fronts occur in fan deltas, quasi-equilibrium fronts develop in most bed forms, and hillslope incisions are just an expression of the tendency of landscape evolution to develop erosional fronts.

Annu. Rev. Fluid Mech. 2010.42:43-66. Downloaded from www.annualreviews.org
by University of California - Berkeley on 02/08/12. For personal use only.

Annu. Rev. Fluid Mech. 2010.42:43-66. Downloaded from www.annualreviews.org
by University of California - Berkeley on 02/08/12. For personal use only.

3. MORPHODYNAMIC EQUILIBRIUM: THE BASIC STATE

The profile of rivers attains equilibrium, adjusting to the function of conveying downstream water and sediment supplied by the watershed. At the basin scale, this is a complex process that falls outside the scope of the present review, as it involves the interaction between the river itself and the adjacent environments (e.g., hillslopes, floodplain, and the ocean) (Sinha & Parker 1996).

However, at the reach scale and for temporal scales short enough that neither subsidence nor tectonic uplift play a significant role, equilibrium is readily understood. In fact, although rivers are not steady systems, their states evolve in response to quasi-steady seasonal forcings punctuated by strong flood fluctuations; however, their longitudinal profiles maintain their shape over geomorphic time; i.e., they have a quasi-equilibrium profile. Hence, let us consider a turbulent plane and unidirectional stream subject to steady forcing, namely given the flow rate and sediment supply. Under these conditions, at morphological equilibrium ($\partial/\partial t = 0$), the Exner equation suggests that the sediment flux per unit width $\mathbf{q}_s$, aligned with the flow, must keep spatially constant: Therefore, recalling Equation 4, the mean bottom stress, as well as the sediment size and the bed slope, must not vary; i.e., the flow must be uniform. This simple result is instructive. In fact, coupling the uniform Chézy law to a bed-load transport relationship for q_s, one readily finds that the equilibrium slope is uniquely determined by the given unit discharge, sediment size, and sediment supply, decreasing monotonically with the former and increasing monotonically with the latter two. Thus, a river responds to an increased sediment supply and/or to bed coarsening by steepening its course, whereas an increased flow discharge drives bottom flattening.

4. QUASI-EQUILIBRIUM PATTERNS: SMALL SCALE

A variety of small-scale patterns arise from instabilities of the uniform equilibrium state. They are beautifully described in early work (Allen 1984). It suffices here to recall that patterns may be subcritical (e.g., ripples, dunes, bed-load sheets) or supercritical (e.g., antidunes, roll waves). Moreover, all these bed forms may be 2D (straight crests) or 3D (curved crests). Fluvial ripples and dunes migrate invariably downstream, whereas antidunes typically (not invariably) migrate upstream. Ripples, dunes, bed-load sheets, and roll waves are strongly asymmetrical (**Figure 3*a***), whereas antidunes are fairly symmetrical.

All the above bed forms have crests orthogonal to the local flow direction. This is not the case for sand ribbons and longitudinal streaks, stationary bed forms exhibiting crests parallel to the main flow (**Figure 3*b***).

4.1. Two-Dimensional Ripples, Dunes, and Antidunes

The theory of small-scale patterns in fluvial streams and the modern field of theoretical morphodynamics stem from a seminal paper (Kennedy 1963) on dune-antidune formation in erodible channels that proposed the basic instability mechanism outlined in Section 2. Later contributions pointed out a number of stabilizing and destabilizing effects (e.g., gravity, suspension, friction, particle inertia, and nonequilibrium bed-load transport). The picture emerging from an early review (Engelund & Fredsøe 1982) can be summarized as follows. Dune instability arises from a balance between the stabilizing effect of gravity and the destabilizing effect of friction (Engelund 1970, Smith 1970). This picture was based (Fredsøe 1974) on a realistic estimate of the longitudinal effect of gravity (Equation 4) coupled with the simplest slip-velocity turbulent closure, which sharply underestimates friction. On the contrary, using a more refined flow model, the destabilizing effect of friction increases sharply, and one is forced to assume an unrealistically large gravitational effect

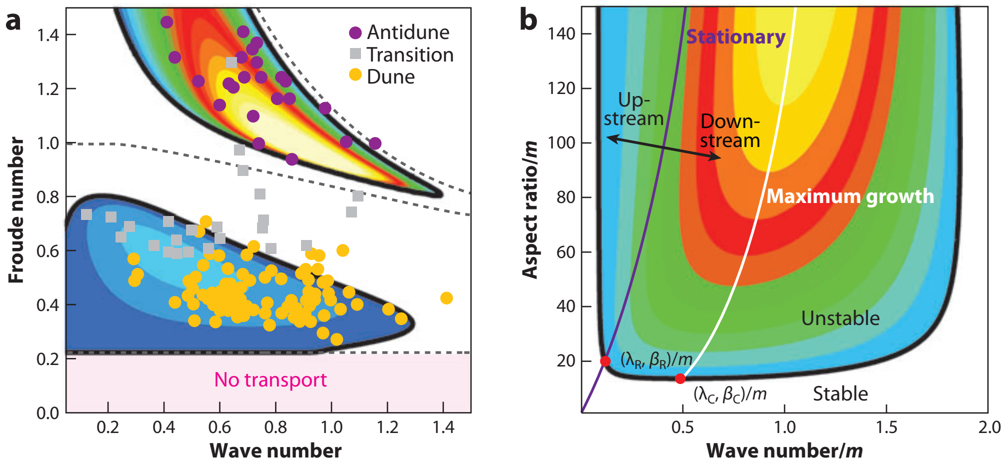

Figure 4

(*a*) Dune instability plot (Colombini 2004), comparing the unstable regions in the Froude-number versus wave-number plane with observations (Guy et al. 1966). The dashed lines correspond to nonmigrating perturbations. (*b*) The unified marginal stability curve for bars of any mode m, showing critical conditions for bar growth and resonant conditions characterized by vanishing speed and vanishing growth rate.

Annu. Rev. Fluid Mech. 2010.42:43-66. Downloaded from www.annualreviews.org by University of California - Berkeley on 02/08/12. For personal use only.

(Richards 1980). Antidune instability turns out not to be significantly affected by gravity; hence a different stabilizing effect (suspension) was invoked to balance the destabilizing effect of friction, but antidunes are known to develop also in the absence of a suspended load. The issue was then not wholly settled.

Progress made since this assessment in 1982 encompasses various lines of research. With regard to the mechanism of dune-antidune instability, some deficiencies of previous linear theories were overcome (Colombini 2004), based on the finding that the phase of the perturbations of shear stress (relative to bed elevation), which drives the instability process, varies rapidly close to the bed. Hence, evaluating the shear stress exerted by the fluid at the top of the saltation layer (as appropriate) rather than at the bed interface (as in previous contributions) introduces an unexpectedly significant effect: The stabilizing role of gravity on bed-load transport is no longer crucial for dune instability, whereas antidune instability is no longer crucially determined by the suspended load. Dunes and antidunes form in the context of an identical conceptual framework, and predictions for the most unstable wavelengths agree satisfactorily with observations in both regimes. **Figure 4*a*** illustrates marginal stability curves bounding two regions of instability, the lower (upper) region corresponding to dune (antidune) instability. The figure also shows vanishing wave speed; dunes are found to migrate downstream, whereas antidunes migrate upstream, in fair agreement with observations.

Later work (Colombini & Stocchino 2005) clarified another issue left open by linear theories: The decoupled approach leads to a resonant behavior (see **Figure 4*b***). The artificial character of this resonance was demonstrated through a coupled potential-flow theory (Coleman & Fenton 2000). However, due to the irrotational assumption, the only unstable region found was a narrow strip adjacent to the resonant line. On the contrary, a fully coupled rotational analysis (Colombini & Stocchino 2005) leads to a fairly conclusive picture: The artificial resonance as well as the near-resonant unstable region disappear, whereas the dune-antidune instability regions are practically unaffected by coupling. At high Froude numbers, however, the existence of fast-moving sediment waves associated with the roll-wave instability emerges only in the context of a coupled approach, confirming results obtained in the framework of shallow-water theories. The roll-wave and antidune modes are simultaneously unstable for sufficiently large values of the Froude number, suggesting that nonlinear effects are responsible for mode competition in that regime.

A third issue, raised to question the actual relevance of linear instability theories (Coleman & Melville 1994), deserves attention. Detailed experimental observations of incipient dune formation in both fine and coarse sand demonstrate the initial development of low-amplitude, short bed forms (sometimes called dune wavelets) with characteristics independent of the Shields stress. These are then subject to a coalescence process whereby larger-amplitude, longer, and stage-dependent dunes eventually develop, in sort of an inverse cascade. It is claimed (Coleman & Melville 1996) that linear theories would be relevant only to explain the formation of dune wavelets associated with the high wave-number peak detected in the growth-rate curve (Richards 1980). This argument is not wholly convincing as this peak corresponds to extremely short perturbations, scaling with bed roughness, which do not fit observations. The relation between these forms and ripples is unclear: They were observed in smooth-transitional regimes (Coleman & Melville 1994). Moreover, the transient character of dune wavelets is also unclear: Coleman & Melville (1994, their figure 4) suggest that dune development reaches a first quasi-equilibrium state, lasting a few minutes, after approximately 200 s from the start of the experiment. This temporary equilibrium then loses stability, and dunes eventually develop. Is the latter process an expression of a secondary bifurcation? The matter needs further work to be settled.

Certainly the role of nonlinearity is crucial to determine the final equilibrium shape of dunes. In the only attempt to view this problem in the framework of stability and bifurcation theory (Colombini & Stocchino 2008), a Landau-Stuart-Hopf amplitude equation was derived for weakly nonlinear dunes (antidunes) within a neighborhood of the maximum (minimum) of the corresponding marginal stability curve. The authors found that tricritical points (i.e., points where the bifurcation shifts from subcritical to supercritical) exist along both marginal stability curves. In situations of practical interest, dune bifurcation is supercritical, and an equilibrium amplitude is reached, whereas antidune bifurcation is subcritical. The authors' conclusion is of conceptual interest: "Dunes of finite, though small, height evolve towards an asymmetric shape and reach an equilibrium amplitude even in the absence of flow separation. The acceleration/deceleration of the flow associated with the sequence of contractions and expansions above the dune is critical in controlling the shape of the bed surface through nonlinear interactions." Criticism is occasionally leveled toward weakly nonlinear theories on the grounds that they would rule out a crucial part of the physics of finite-amplitude flow perturbations, namely separation at the dune crest. This would be justified if separation were an essential feature of dune formation. On the contrary, "low-angle dunes are common and may often represent the most abundant dune shape: it appears increasingly likely that many large rivers are characterized by dunes with leeside slopes lower than the angle of repose" (Best 2005). In other words, even in the fully developed regime, separation is not an essential feature of dunes. Conversely, it is well-known that flow does not separate from the crests of antidunes.

This notwithstanding, separating dunes are an equally common bed form and pose a quite interesting and challenging problem, which has been investigated both experimentally and numerically. The first sound model for the flow past a train of fully developed dunes (McLean & Smith 1986) has been followed by a number of numerical contributions using various turbulent closures to model a quite complex flow structure, including a separation zone forming on the leeside, a free shear layer developing at the boundary between the separation zone and the free stream, a wake region growing and dissipating downstream, and an internal boundary layer growing downstream of the reattachment zone. Parallel to numerical simulations, increasingly detailed laboratory investigations of flow past fixed bed dunes (Best 2005) have provided useful data. Recent successful attempts to incorporate this knowledge into a rational morphodynamic

Annu. Rev. Fluid Mech. 2010.42:43-66. Downloaded from www.annualreviews.org by University of California - Berkeley on 02/08/12. For personal use only.

framework (Giri & Shimizu 2006) have employed an advanced closure scheme, a computational grid sufficiently refined in the near-bed region, and a correct free-surface condition (no rigid lid). The latter simulations were also able to reproduce the initial formation of dune wavelets and their coalescence into longer and slower fully developed dunes, with wavelengths and amplitudes comparing reasonably with observations.

Sorting: the process whereby particles of different sizes arrange spatially into sequences of coarser and finer patches

4.2. Dune Superimposition and Amalgamation

Smaller amplitude dunes (or ripples) are commonly observed on the stoss side (and often on low-angle leesides) of larger dunes. The migration of these forms, sometimes called sand sheets (Venditti et al. 2005a), over larger dunes is the cause of pronounced temporal fluctuations of sediment transport observed at the dune leeside. Moreover, the interaction of a dune with an upstream faster-moving companion may lead to amalgamation, the new pattern having a height lower than that obtained from a simple superposition of the two original bed forms. Again, the mechanistic basis of coexisting patterns of different scales has not been investigated. Qualitative suggestions propose that they might be a response to nonuniform and unsteady flow, as well as of hysteresis effects within a flood hydrograph (Best 2005). However, this interpretation conflicts with the observation (Venditti et al. 2005a) that sand sheets may coexist with dunes under steady conditions.

Annu. Rev. Fluid Mech. 2010.42:43-66. Downloaded from www.annualreviews.org
by University of California - Berkeley on 02/08/12. For personal use only.

4.3. Three-Dimensional Dunes

The issue of why and when 3D dunes form is unsettled. This applies, in particular, to the peculiar pattern of the so-called Barkhan dunes observed also under supply-limited conditions. Laboratory observations suggest that, in a sufficiently wide channel and provided the experiment is long enough, 2D dunes evolve invariably into 3D patterns. More precisely, "once 2D bedforms are established, minor, transient excesses or deficiencies of sand are passed from one bed form to another. The bed-form field appears capable of absorbing a small number of such defects but, as the number grows with time, the resulting morphological perturbations produce a transition in bed state to 3D forms that continue to evolve, but are pattern-stable. The 3D pattern is maintained by the constant rearrangement of crestlines through lobe extension and starving downstream bedforms of sediment, which leads to bifurcation" (Venditti et al. 2005b). Surprisingly, no published stability theory is available to check the existence of a morphodynamic Squire theorem whereby dune perturbations with spanwise structure would be less unstable than their 2D counterparts.

4.4. Sand Ribbons and Sand Streaks

Sand ribbons appear in the form of long, parallel streaks of sand aligned with the channel axis characterized by regular-spacing scaling with flow depth. It has long been speculated that this might be a rare example of hydrodynamically forced bed-form instability, triggered by sidewall vortices that would excite bottom perturbations that would then propagate away from the walls. The need for a sidewall forcing mechanism was associated with the idea that small, longitudinally uniform, spanwise perturbations could not be linearly excited spontaneously in an infinitely wide channel, as a laterally and longitudinally uniform basic state provides no coupling with linear perturbations of axial vorticity. However, this is only true if turbulence anisotropy is neglected. On the contrary, it has been conclusively shown (Colombini 1993) that, allowing for anisotropy, coupling arises and turbulence-driven secondary flows are able to sustain the growth of sand-ribbon perturbations. The latter instability is reinforced by sorting in heterogeneous sediments (Colombini & Parker 1995) (**Figure 3*b*,*c***).

Annu. Rev. Fluid Mech. 2010.42:43-66. Downloaded from www.annualreviews.org
by University of California - Berkeley on 02/08/12. For personal use only.

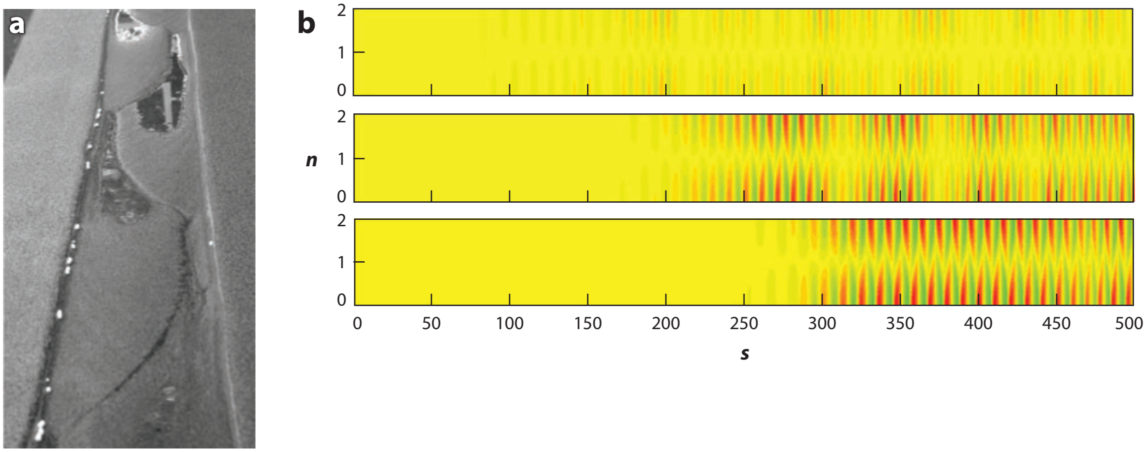

Figure 5

(*a*) Alternate bars observed in the laboratory. Figure courtesy of W. Bertoldi. (*b*) Numerical simulations (Federici & Seminara 2003) of the development of alternate bars show the convective nature of bar instability. Persistent perturbations localized at the initial cross section generate wave groups that reach asymptotically an equilibrium amplitude.

5. QUASI-EQUILIBRIUM PATTERNS: MESOSCALE

Mesoscale patterns, called bars, have wavelengths scaling with channel width and heights scaling with flow depth. Free bars form in straight or weakly curved channels and display themselves in the form of migrating alternate sequences of pools and riffles separated by diagonal fronts. They may be arranged in single rows (alternate bars) in sufficiently narrow channels (Callander 1969) (**Figure 5**) or in multiple rows in sufficiently wide channels, where they give rise to the development of braiding patterns (Fujita & Muramoto 1985) (**Figure 2*b***). Bars may also be forced by various mechanisms: Curvature in meandering channels determines rhythmic sequences of pools at the outer bend and riffles at the inner bends (**Figure 2**); flow divergence promotes the formation of central bars and a tendency of the stream to bifurcate; and nonuniform boundary conditions (**Figure 6**) force the spatial development of nonmigrating bars, otherwise quite similar to free bars.

5.1. Free Bars

Pool: deep part of the cross section of a river; pools are stationary in outer bends but may migrate when associated with bed forms

Braiding rivers: river morphology consisting of an interconnected network of curved channels separated by migrating bars

Given their scaling, the hydrodynamics of free bars can be adequately modeled using the shallow-water equations. The subject is fairly settled (Tubino et al. 1999). In a classical normal-mode analysis, the number of rows of bar perturbations is represented by the order m of the lateral Fourier mode, with $m = 1$ corresponding to single-row (alternate) bars: Both odd and even modes satisfying the no-flux condition at the sidewalls are allowed. A linear instability theory then leads to an algebraic dispersion relationship of the form (Blondeaux & Seminara 1985)

$$\omega = N\frac{-\lambda^4 + in_3\lambda^3 + n_2\lambda^2 + in_1\lambda + n_0}{\lambda^3 + id_2\lambda^2 + d_1\lambda + id_0} = \omega(\lambda; \beta, \tau_* d_s). \tag{8}$$

Here, λ is the dimensionless real longitudinal wave number scaled by the channel half-width; ω is the dimensionless complex growth rate; and coefficients of Equation 8 are functions of the dimensionless parameters characteristic of the basic state, namely the aspect ratio β, the Shields stress of the basic uniform flow τ_*, and the ratio of grain size to flow depth d_s. Equation 8 applies

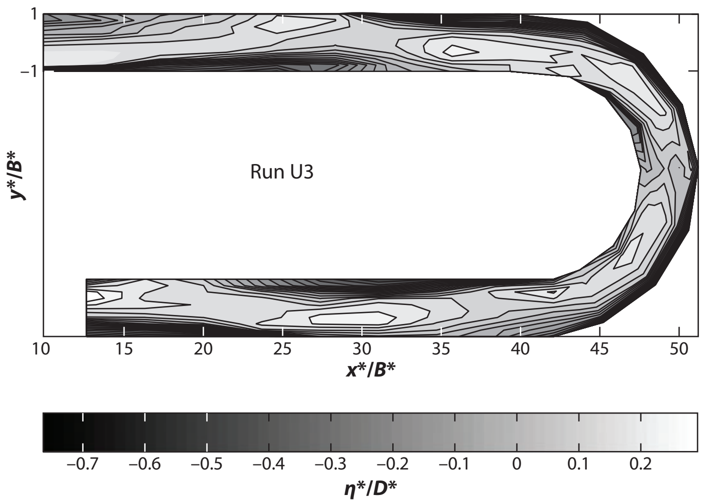

Figure 6

Laboratory observations (Zolezzi et al. 2005) of bottom perturbations in the straight reaches located downstream and upstream of a 180° bend reveal that morphodynamics influence both the downstream and the upstream reach in superresonant channels. Flow direction is clockwise.

Annu. Rev. Fluid Mech. 2010.42:43-66. Downloaded from www.annualreviews.org
by University of California - Berkeley on 02/08/12. For personal use only.

to any mode m, provided λ, β, and ω are replaced by λ/m, β/m, and ω/m, respectively. This suggests that the actual scale appropriate to mode m is a factor m smaller than the channel width. Recognizing β as control parameter for bar instability (for given values of τ_* and d_s), one finds that instability occurs above a threshold value (β_c) of the control parameter with the most unstable wave number (λ_c). The threshold condition depends on the dominant form of sediment transport. For dominant bed load, (*a*) the value of β_c ranges from about 5 to 6; (*b*) the most unstable wavelength ranges typically about six channel widths; and (*c*) the bar speed varies along the marginal stability curve (e.g., it is positive at critical conditions, decreases for increasing β along the left branch of the curve, and vanishes at $\beta = \beta_R$ to become negative for values of $\beta > \beta_R$) (**Figure 4*b***). We note that the point (β_R, λ_R) defines a free response of the bed in the form of stationary alternate bars: In a sinuous channel, curvature forces essentially the same response, an observation at the basis of the resonance-driven bend instability theory of meander formation (Blondeaux & Seminara 1985, Seminara 2006). Similar results are found when suspended load is dominant (Federici & Seminara 2006, Tubino et al. 1999) although bars form more easily (lower β_c) and lengthen (lower λ_c). Linear results are in fair agreement with laboratory and field observations (Colombini et al. 1987).

The physical mechanism of bar instability is of the type discussed in Section 2. Here, the major destabilizing effect is friction, whereas the lateral effect of gravity plays a stabilizing role. Recalling Equation 4, it is not surprising to find that the stabilizing effect increases as τ_* decreases and/or m increases, which explains why higher-order modes are excited for increasingly higher values of the control parameter. The effect of suspended load depends on the ratio of the particle-settling distance to the bar wavelength and turns out to be destabilizing (stabilizing) in the small (high) wave-number range.

Nonlinearity adds a number of important features. Landau (Colombini et al. 1987) and Ginzburg-Landau (Schielen et al. 1993) evolution equations, derived for the amplitude of weakly nonlinear alternate bars, show that periodic equilibrium solutions bifurcate supercritically; nonlinear bars tend to form diagonal fronts and migrate more slowly than linear bars; and the group velocity of meander trains is larger than their phase speed (anomalous dispersion) (Schielen et al. 1993). Equilibrium amplitudes can thus be predicted theoretically and compare reasonably well with laboratory observations. Strongly nonlinear results, obtained through numerical solutions of the fully nonlinear problem (Federici & Seminara 2003, 2006), confirmed the convective nature of bar instability (**Figure 5**) and showed that nonlinearity lengthens and slows down (by a factor of one-third to one-fourth) linear bars. As bars develop in space, care must be taken in interpreting laboratory observations, which likely depend on the size of the experimental facility. The nonlinear evolution of higher-order modes into braiding has been investigated experimentally in a fundamental paper (Fujita & Muramoto 1985) that found that the higher-order modes selected in the initial stage coalesced into lower-order patterns (again an example of an inverse cascade), which then amplified until the bed emerged and the initial multiple-row bar pattern evolved into an interconnected network of curved channels separated by no-longer-active bars. This process awaits a full interpretation.

Point bar: stationary sediment deposits typically located at inner bends

Annu. Rev. Fluid Mech. 2010.42:43-66. Downloaded from www.annualreviews.org
by University of California - Berkeley on 02/08/12. For personal use only.

5.2. Bars Forced by Curvature

In meandering rivers, a distinct process occurs: the formation of stationary, rhythmic sequences of riffles and pools associated with channel curvature. Various factors contribute to this process. First, the centripetal acceleration of fluid particles moving along curvilinear trajectories cannot be simply provided by the (vertically uniform) lateral pressure gradient established by a lateral slope of the free surface. Hence a centrifugal secondary flow, directed outward close to the free surface and inward close to the bed, is needed to provide the excess (defect) of centripetal force required in the upper (lower) part of the cross section. We let C_0, D_0, L, and r_0 denote the characteristic values of flow conductance, flow depth, meander wavelength, and radius of curvature of channel axis, respectively. Then, the intensity of this secondary flow is $O(\delta)$, the parameter δ ($\equiv C_0 D_0/r_0$) measuring the intensity of centripetal effects relative to dissipation. Mild (sharp) bends are then such that $\delta \ll 1$ ($\delta \gg 1$).

If the bed is nonerodible, a free-vortex effect prevails initially, with shorter longitudinal trajectories in the inner part of the bend than in the outer part. As a result, flow at the inner bend accelerates relative to the outer bend, a purely metric effect with intensity measured by the parameter B/r_0 with B channel width. Hence, for a given channel curvature, metric effects decrease in narrow bends. Conversely, for a given channel width, metric effects are enhanced in strongly curved bends. Proceeding downstream, the secondary flow generates a net outward transfer of momentum, and the thread of high velocity progressively moves outward. However, for convective transfer to be effective, the basic longitudinal flow must have a lateral dependence. This is a second-order effect in the context of linear models, where perturbations are sought in a neighborhood of a uniform basic state.

Bed erodibility modifies this picture, as secondary flow acts also on grain particles, which are forced to deviate from the longitudinal direction. Sediment is then transported toward the inner bends where a point bar builds up at the expense of the outer bends where pools develop. As a result, a topographical component of the secondary flow is generated, which is dominant in finite-amplitude bends (Dietrich & Smith 1983) and drives an additional contribution to sediment transport and bed topography. The continuity equation suggests that the intensity of this topographic steering is $O(\lambda)$ ($\equiv 2\pi B/L$). Hence, a long (short) bend generates a fairly weak (strong) topographically induced secondary flow.

However, in mild and long erodible bends, the perturbations of bed topography are by no means necessarily small relative to the average flow depth. In fact, an estimate of the lateral bed slope is readily obtained, with the stipulation that the lateral component of the sediment flux q_n

vanishes, a condition strictly valid for fully developed flow and topography in constant-curvature channels. From Equation 4, one readily finds that the relative amplitude of bed perturbations is $O(\gamma)$ with $\gamma \equiv \beta\sqrt{\tau_*}(\delta, \lambda)$. Hence, mild ($\delta \ll 1$) and long ($\lambda \ll 1$) bends may be nonlinear as long as the aspect ratio of the channel is sufficiently large ($\beta \gg 1$) and the Shields stress is not too small.

Morphodynamic influence: process whereby the presence of any morphological constraint (e.g., a bend) may be felt upstream and/or downstream

The tools usually employed to relax the linear constraint are typically numerical. And, indeed, numerical models have been proposed to predict flow and bed topography in meandering channels with finite curvature and arbitrary width variations. However, sufficiently mild and long bends are amenable to a nonlinear analytical treatment taking advantage of a slowly varying assumption (Bolla Pittaluga et al. 2009). The basic idea is to allow for finite-amplitude bed deformations in the basic state, assuming that the basic flow is a locally uniform flow in a channel with an unknown, albeit slowly varying, shape of the cross section. An expansion of the solution in powers of δ then brings at first order the crucial role of momentum redistribution driven by the lateral structure of the basic state. The analysis leads to a nonlinear integro-differential equation for bed elevation, which can be solved for given channel geometry. Results for a periodic train of so-called sine-generated meanders, characterized by the sinusoidal distribution of channel curvature, can be compared with outcomes of linear theories (Blondeaux & Seminara 1985), showing interesting features, which are discussed in the next section.

Annu. Rev. Fluid Mech. 2010.42:43-66. Downloaded from www.annualreviews.org
by University of California - Berkeley on 02/08/12. For personal use only.

5.3. Stationary Bars as Vectors of Morphodynamic Influence

Let us now pose a fundamental question that can be illustrated by a constant-curvature erodible bend connected to straight reaches located both upstream and downstream. A bar-pool system develops in the bend and determines a nonflat stationary bed profile at the initial cross section of the downstream straight reach: How does the downstream reach respond to this boundary condition? In other words, does the presence of the bend exert a morphodynamic influence downstream? Similarly, how does the bar-pool system merge into the uniform configuration of the straight reach upstream? Does the presence of the bend exert a morphodynamic influence upstream?

A linear answer to these questions is contained in the dispersion relationship (Equation 8) showing that a uniform turbulent open-channel flow over an erodible bottom is also able to support linear stationary (i.e., nonmigrating) bars, which do not amplify/decay in time but may amplify/decay in space. Their characteristics are obtained by allowing λ to be complex and setting ω to vanish in the dispersion relationship. For each lateral mode m, four solutions for the complex wave number λ are obtained (Olesen 1983). Typically, two of them describe nonoscillatory spatial perturbations that decay fairly fast. The other two solutions describe oscillatory spatial perturbations that decay more slowly, spreading their influence over a significant length. A careful examination of these solutions reveals that their signs change, for each mode m, as a threshold value β_{Rm} of the aspect ratio of the channel is exceeded. The picture that emerged (Zolezzi & Seminara 2001) may be summarized stating that perturbations of bed topography are felt only downstream in sufficiently narrow channels with $\beta < \beta_{R1}$ (subresonant channels), whereas they significantly affect the upstream reach in wider channels, such that $\beta > \beta_{R1}$ (superresonant channels). The latter findings have been confirmed (Zolezzi et al. 2005) by laboratory observations (**Figure 6**). When a significant fraction of sediments is transported in suspension, the resonant values of the aspect ratio decrease (Federici & Seminara 2006).

In the nonlinear regime, the indefinite growth of the exponentially growing mode is inhibited, and an equilibrium amplitude is asymptotically reached. This has been shown by a weakly nonlinear theory of stationary bars valid in a neighborhood of the resonant conditions (Seminara & Tubino 1992).

Annu. Rev. Fluid Mech. 2010.42:43-66. Downloaded from www.annualreviews.org
by University of California - Berkeley on 02/08/12. For personal use only.

6. QUASI-EQUILIBRIUM PATTERNS: LARGE SCALE

We now consider the response of the equilibrium state to long perturbations, distinguishing between perturbations of bed elevation and planform perturbations.

6.1. Free Patterns: Bed Forms

Let us consider uniform free-surface flow in a straight rectangular channel, with a cohesionless bottom of uniform grain size, constant width, slope, and discharge. We denote the associated uniform flow depth by D_0, speed by U_0, sediment flux per unit width by q_{s0}, Froude number by F_0, and flow conductance by C_0. Linear perturbations of this basic state in the form of 1D normal modes satisfying de Saint Venant and Exner governing equations obey the following dispersion relationship (Lanzoni et al. 2006):

$$i\omega^3 - 2\omega^2(i\lambda + 1) - i\omega\left\{i\lambda[3 + \Gamma(c_M - 1)] - \lambda^2\left[1 - \frac{1}{F_0^2} - \frac{\Gamma c_M}{F_0^2}\right]\right\} + i\lambda^3\frac{\Gamma}{F_0^2} = 0. \quad (9)$$

Here Γ is a dimensionless parameter proportional to the ratio t_H/t_M between hydrodynamic and morphodynamic timescales, hence a typically small parameter except close to the critical conditions; λ is the dimensionless wave number scaled by $l_0 = C_0^2 D_0$; and ω is the dimensionless angular frequency of the perturbation, scaled by l_0/U_0. The above relation defines, in general, three complex eigenmodes, $\omega_j (j = 1, 2, 3)$. Assuming that λ and F_0 are finite and expanding ω_j in powers of Γ (decoupled approach) at leading order, one finds a classical result: One of the eigenvalues vanishes, and the remaining two reduce to those found in the fixed bed case. The former is associated with perturbations that are invariably stable and migrate downstream; the latter is unstable for $F_0 > 2$ and perturbations migrate downstream: This mode describes the classical roll-wave instability. At the next order, small morphodynamic corrections for the two hydrodynamic modes and a third morphodynamic nontrivial mode arise. This is invariably stable and upstream (downstream) migrating under supercritical (subcritical) conditions. However, in the short wave limit ($\lambda \to \infty$), both the wave speed and the negative growth rate of the morphodynamic mode become unbounded as $F_0 \to 1$, a consequence of the decoupled approach becoming singular in this limit. This singularity can be removed by coupling hydrodynamics and morphodynamics, through an expansion in suitable powers of Γ in a neighborhood of criticality (Lanzoni et al. 2006). Under supercritical conditions, the morphodynamic mode may be unstable and migrates downstream. A very weak instability of this kind had been previously detected numerically (Lyn & Altinakar 2002).

The nonlinear evolution of 1D perturbations was investigated numerically by means of a quasi-conservative fully coupled algorithm (Siviglia et al. 2008). In particular, the nonlinear response to an initial short bottom perturbation (a hump) subject to a supercritical flow deviates from the linear one: The linear growth predicted by the coupled linear theory does not persist in the nonlinear regime; the morphodynamic influence is felt both upstream and downstream through the formation of a secondary hump migrating downstream; and nonlinearity gives rise to wave peaking. Similar features arise in the subcritical regime. On the contrary, long subcritical perturbations in the nonlinear regime do not differ significantly from linear perturbations: No secondary hump is generated, and nonlinearity is unable to produce sharp fronts.

Of greater interest is the response of an erodible bed to the propagation of hydrodynamic fronts. Experimental observations (Bellal et al. 2003) suggest that the propagation of a hydraulic jump on an erodible bed undergoes two stages. Initially the jump migrates fairly fast and is unable to excite a significant morphodynamic response. Later the jump has slowed down sufficiently for

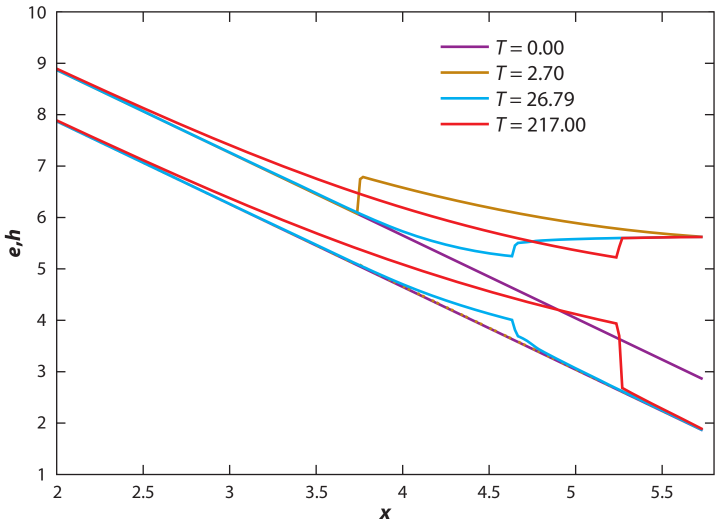

Figure 7

Nonlinear morphodynamic response to the propagation of a hydraulic jump (Siviglia et al. 2008). The jump overshoots the location where a steady jump would exist on a fixed bed ($F_0 = 1.27$, $\Gamma = 0.04$, $C_0 = 18.3$).

Annu. Rev. Fluid Mech. 2010.42:43-66. Downloaded from www.annualreviews.org
by University of California - Berkeley on 02/08/12. For personal use only.

hydrodynamic and morphodynamic timescales to be comparable. At this stage, a sediment front is generated by the sharp reduction of the transport capacity of the stream through the hydraulic jump. The front then migrates downstream, and progressively the hydraulic jump disappears, leading to a final uniform equilibrium state. This picture is perfectly reproduced by numerical simulations (**Figure 7**).

6.2. Free Patterns: Planforms

Erodible channels respond to bank erosion by propagating planform waves, which, in meandering rivers, consist of variations of channel alignment. The framework employed to predict the planform evolution (Ikeda et al. 1981) is based on the stipulation that the channel, identified through its centerline, moves in the normal direction with a migration speed ζ. The following nonlinear integro-differential equation is then found to govern planform evolution (Seminara et al. 2001):

$$\frac{\partial \theta}{\partial t} - \frac{\partial \theta}{\partial s} \int_0^s \zeta \frac{\partial \theta}{\partial s} ds = \frac{\partial \zeta}{\partial s}, \tag{10}$$

where θ (s, t) is the angle that the local tangent to the channel axis forms with the valley axis, and s is the intrinsic longitudinal coordinate. The mathematical formulation of planform evolution is completed once an erosion law is established to relate the migration speed ζ to the stream hydrodynamics. Formulating an appropriate integrated and a continuous description of the actually intermittent process of bank collapse and sediment removal from the bank foot (Darby et al. 2002) is a quite complex problem, which still requires attention. A simple rule that has had an enormous impact on the field (Ikeda et al. 1981) is based on the assumption, somehow substantiated by field observations, that an appropriate measure of lateral migration is the differential excess of flow speed at the outer and inner banks, the implication being that the material eroded at outer banks is redeposited at inner bends, as observed in the field.

Neck cutoff: process occurring when the planform evolution of meandering rivers leads two branches of a meander loop to merge

Meander formation is then explained through a planform stability analysis, assuming a straight basic configuration and investigating the conditions for the growth of small normal-mode perturbations of the type $\theta_1 \exp i(\lambda s - \omega t)$. As assessed in a recent survey paper (Seminara 2006), a number of features emerge. Small-amplitude meanders behave as linear oscillators, which resonate for values of wave number λ and aspect ratio β, equal to λ_R and β_R, respectively. Hence, at the linear level, the free stationary bar discussed in Section 5 is resonantly excited by curvature. Moreover, meander bends migrate, and migration is driven by a phase lag between bank erosion and curvature. As in any linear oscillator, the phase lag changes sign at resonance; hence subresonant meanders ($\beta < \beta_R$) migrate downstream, whereas superresonant meanders migrate upstream. The nonlinear planform evolution of the selected mode displays a number of characteristics observed in the field: Regular meander trains are typically upstream (downstream) skewed under subresonant (superresonant) conditions; the lateral migration increases to a peak and then decreases; meander speed decreases monotonically; and development leads to neck cutoff, i.e., the merging of adjacent meander branches. Numerical simulations, pursued beyond cutoff (Camporeale et al. 2005, Frascati & Lanzoni 2009), suggest that the repeated occurrence of neck cutoffs leads to a statistically stationary state, such that channel sinuosity (i.e., the ratio between intrinsic and Cartesian lengths) displays small oscillations around an asymptotically constant value (**Figure 8**).

Nonlinearity (Bolla Pittaluga et al. 2009) essentially confirms the linear picture (**Figure 9**). Bend instability still selects a meander wave number increasing with the aspect ratio β, although nonlinearity damps strongly the resonant excitation of stationary free bars. Upstream migration is confirmed above a threshold value of the aspect ratio β quite close to the resonant value of the linear theory.

7. A GLANCE AT EROSIONAL AND DEPOSITIONAL PATTERNS

Although space does not allow a discussion of erosional and depositional patterns in detail, we touch upon this subject to introduce the reader to a fascinating research field that is likely to play an increasingly important role in the century of global warming.

7.1. Landscape Evolution Models and the Geomorphologic Peclet Number

The mechanics of landscape evolution stems from a seminal study (Smith & Bretherton 1972) of the incipient development of erosional rills. Ridge-and-valley topography exhibiting a distinct characteristic wavelength is observed in soil-mantled landscapes (**Figure 1*a***), and submarine and even Martian environments (Perron et al. 2008). To investigate the formation of ridge-and-valley topography, Perron et al. (2008) coupled the evolution equation (Equation 2), with $\mathcal{S} = \mathcal{D} = 0$ and $\nabla \cdot \mathbf{q}_s$ given by Equation 6, with an appropriate description of overland flow on a steep topography. The shear stress in the channelized portion of the landscape was obtained, evaluating the local flow rate in terms of the associated drainage area A. Hence the landscape evolution, affecting A, has a feedback on the hydrodynamics, which in turn affects the detachment rate. The output was the derivation of a "nonlinear advection-diffusion equation in which the quantity being advected and diffused is elevation" (Perron et al. 2008):

$$\eta_{,t} = D_m \nabla^2 \eta - K(A^{\mu} |\nabla \eta|^n - \tau_c^*) + U, \tag{11}$$

with K, μ, and n as positive parameters. Diffusion naturally tends to smooth perturbations of bed elevation. Advection drives their nonlinear propagation across the landscape in the direction of

Annu. Rev. Fluid Mech. 2010.42:43-66. Downloaded from www.annualreviews.org
by University of California - Berkeley on 02/08/12. For personal use only.

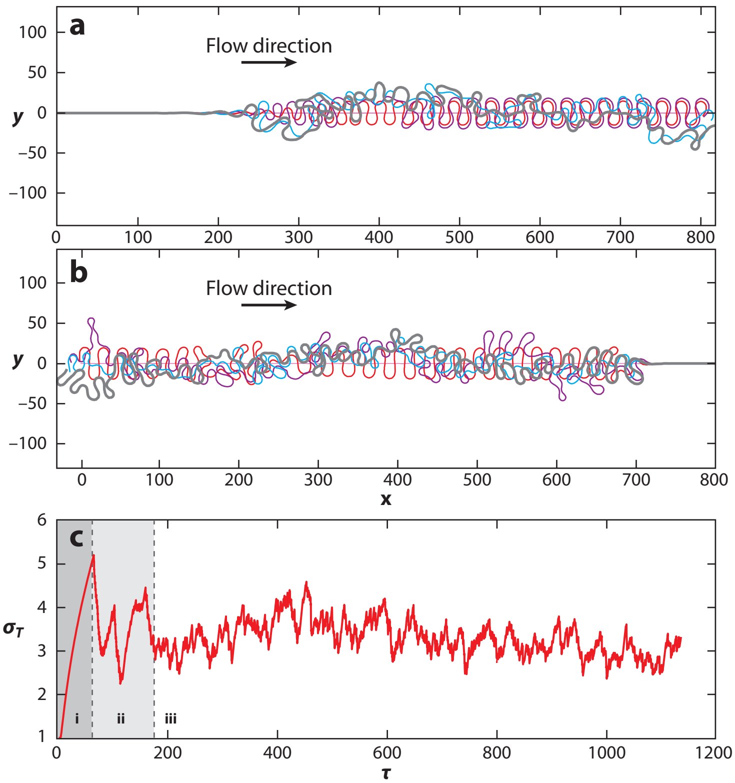

Figure 8

The response of the planform of an erodible channel to small random perturbations of an initially straight configuration (Lanzoni et al. 2006) reveals the convective nature of meander instability. Simulations were carried out imposing no constraint at the channel ends. (*a*) Under subresonant conditions, wave groups migrate downstream, leaving the upstream reach unperturbed. (*b*) Under superresonant conditions, wave groups migrate upstream, leaving the downstream reach unperturbed. Note the capacity of the model to generate multiple loops as well as downstream and upstream skewing of single meanders as observed in nature. (*c*) The temporal evolution of the planform sinuosity displays three stages. (*i*) An initial unnatural pattern regularity promotes a monotonic increase of sinuosity up to an incipient cutoff. (*ii*) The cutoff destroys regularity, and sinuosity decreases tending toward a stationary state. (*iii*) A stationary state punctuated by fluctuations arises as a result of irregularly repeated cutoff events (Frascati & Lanzoni 2009).

Annu. Rev. Fluid Mech. 2010.42:43-66. Downloaded from www.annualreviews.org
by University of California - Berkeley on 02/08/12. For personal use only.

the topographic gradient vector. Tectonic uplift is a crucially important source term that feeds steadily the evolution process.

Numerical solutions of Equation 11 (**Figure 10**) show that the evolution process is crucially controlled by a geomorphologic Peclet number (Pe) measuring the ratio between the contributions of advection and diffusion. For small Pe, valleys are barely detected in a steep ridgeline. At intermediate values of Pe, first-order valleys form, which narrow as Pe increases further. For large Pe, the valley spacing reaches a minimum. It then begins to increase again because the valleys branch, forming tributaries. At still higher values of Pe, the trend is again reversed, with branching valleys becoming more narrowly spaced.

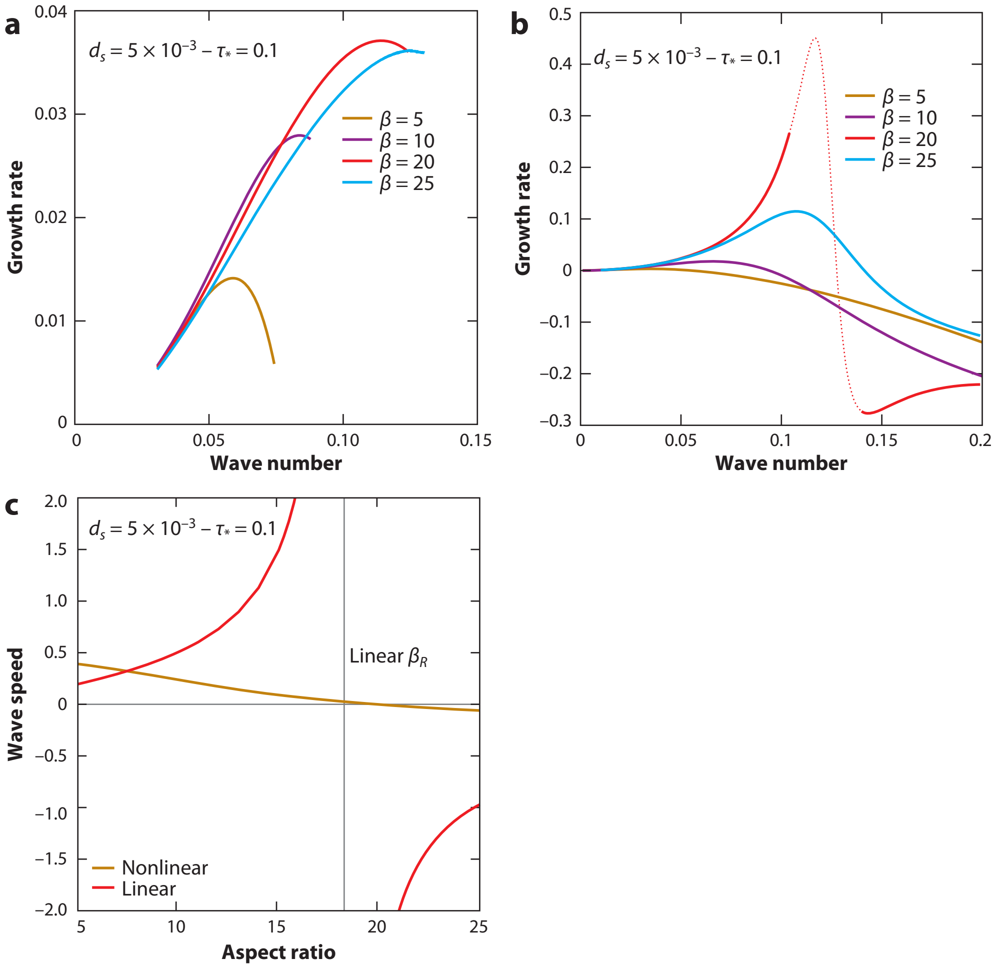

Figure 9

Comparison between the (*a*) nonlinear and (*b*) linear response for a periodic train of sine-generated meanders, showing the crucial role of nonlinear damping in a neighborhood of resonance (Bolla Pittaluga et al. 2009). (*c*) Upstream meander migration is also confirmed above a threshold value of the aspect ratio β quite close to the resonant value β_R of the linear theory.

7.2. Delta Evolution and Avulsions

Natural deltas build up and evolve through various mechanisms. Sediment deposition, driven by the abrupt flow deceleration at the outlet, causes the delta to tend to prograde seaward, a process accompanied by a sequence of avulsions dissecting the fan shape. Progradation is counteracted by subsidence (due to sediment compaction) and sea-level rise. The balance between these two major effects is quite delicate and determines the survival of coastal wetlands, environments of special ecological values. In particular, this equilibrium may be disrupted by anthropogenic actions. A prototypical example is the construction of extensive levees on the lower Mississippi River. Although they protect the city of New Orleans and prevent the river from avulsing upstream, levees have cut sediment replenishment to the delta. As a result, marshlands are sinking into the sea, and the shoreline is rapidly eroding. Modeling the evolution of deltas on geomorphic timescales is then a hot subject, as yet to be fully explored. What is actually needed, however, is a theory

Avulsion: process whereby a river abandons its course in favor of a new path

Annu. Rev. Fluid Mech. 2010.42:43-66. Downloaded from www.annualreviews.org by University of California - Berkeley on 02/08/12. For personal use only.

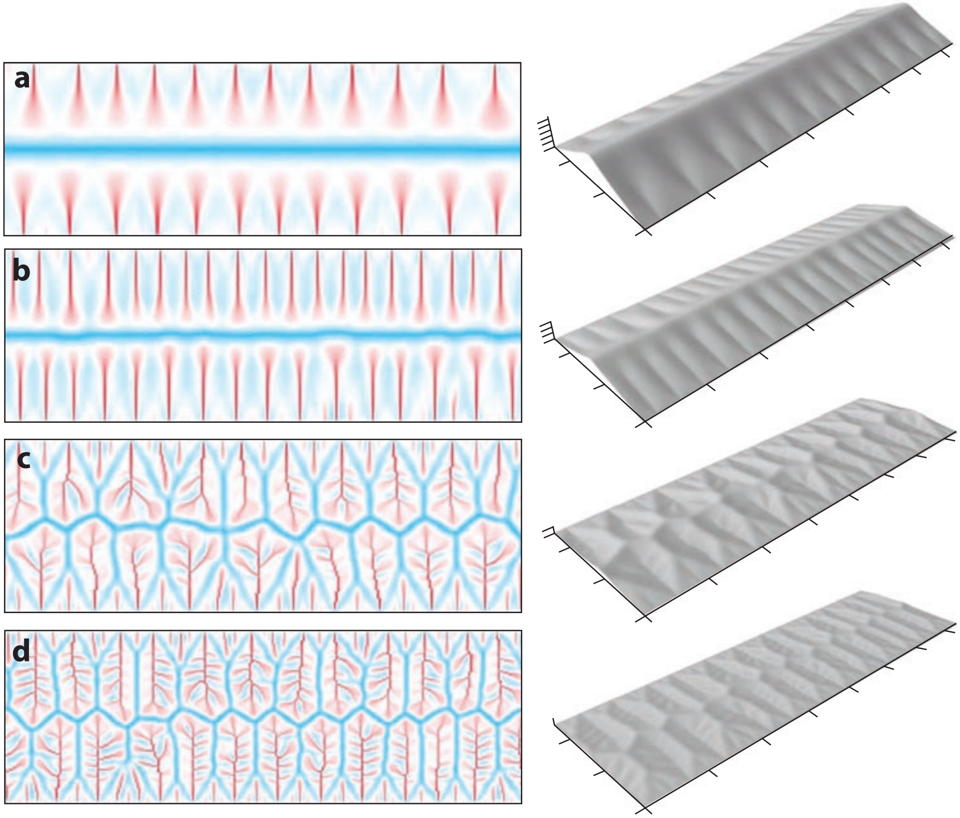

Figure 10

Landscapes obtained by a numerical simulation model (Perron et al. 2008), with four types of patterns emerging. (*Left column*) Image maps, showing the normalized Laplacian of elevation, with concave-up areas (valleys) in red and concave-down areas (hillslopes) in blue. (*Right column*) Perspective views, with axis tick intervals of 200 m in the horizontal and 5 m in the vertical direction. Vertical exaggeration is 4 ×. Figure courtesy of J.T. Perron.

of the wider class of depositional patterns, called alluvial fans (Parker et al. 1998). The peculiar feature of these patterns is that, along with the bed interface, the free unknown boundary also includes the moving front of the fan. At the foreset-bottomset break, the shoreline migration can be specified in terms of a shock condition derived in a similar context (Swenson et al. 2000). Various further elements are needed (Parker & Sequeiros 2006): In particular, sand-bed rivers carry typically far more mud than sand; sand is transported as bed load and can be exchanged with the bed, whereas mud can only settle in the floodplain. Some progress has been made with the help of a laterally averaged formulation based on empirical assumptions on flow and sediment repartition between channelized and unchannelized portions of the delta (Parker & Sequeiros 2006). **Figure 1*b*** shows the degree of success of such a land-building model. The satellite photograph displays the predicted front of the Wax Lake delta (Louisiana) out to year 2081. The great future challenge will be to construct a theory of the development of delta networks that can display the crucial role played by avulsions. Such a model will also have to include a quantitative description of the trapping rate of mud in the delta, accounting for the important role of vegetation, as well as the mechanisms of the removal of delta sediment offshore.

Annu. Rev. Fluid Mech. 2010.42:43-66. Downloaded from www.annualreviews.org
by University of California - Berkeley on 02/08/12. For personal use only.

Annu. Rev. Fluid Mech. 2010.42:43-66. Downloaded from www.annualreviews.org
by University of California - Berkeley on 02/08/12. For personal use only.

FUTURE ISSUES

1. Researchers need to incorporate the current knowledge of near-wall hydrodynamics into models of sediment entrainment by clarifying the spatial-temporal distribution of the occurrence and intensity of near-wall coherent structures under rough-wall conditions, developing a sound mechanical model of particle entrainment by single near-wall events, understanding the feedback of sediment transport on near-wall turbulence, and clarifying the hydrodynamics of particle collision.
2. The present theories of small-scale patterns should be extended to cover 3D perturbations as well as nonlinear mode interactions to clarify the origin of the inverse cascade observed in experiments.
3. A theory of network formation in depositional environments and braiding rivers needs to be developed to account for the role of avulsions.
4. The mechanisms of erosion and supply-limited sediment transport responsible for the development of patterns in rocky environments should be explored.

DISCLOSURE STATEMENT

The author is not aware of any affiliations, memberships, funding, or financial holdings that might be perceived as affecting the objectivity of this review.

ACKNOWLEDGMENTS

I would like to thank my colleagues M. Colombini, M. Bolla Pittaluga, and N. Tambroni (DICAT, Genova University) for many useful discussions and help in preparing this article. I also thank W. Bertoldi, B. Federici, J. Kirchner, S. Lanzoni, G. Parker, J. Perron, and A. Siviglia for providing original figures. This work has been funded by CARIVERONA (Progetto MODITE).

LITERATURE CITED

Allen JRL. 1984. *Sedimentary Structures: Their Character and Physical Basis*. Amsterdam: Elsevier

Bellal M, Spinewine B, Savary C, Zech Y. 2003. Morphological evolution of steep-sloped river beds in the presence of a hydraulic jump: experimental study. *Proc. 30th IAHR Congr., Int. Assoc. Hydraul. Res.*, ed. C Theme, pp. 133–40. Greece: Thessaloniki

Best J. 2005. The fluid dynamics of river dunes: a review and some future research directions. *J. Geophys. Res.* 110:F04S02

Blondeaux P, Seminara G. 1985. A unified bar-bend theory of river meanders. *J. Fluid Mech.* 157:449–70

Bolla Pittaluga M, Nobile G, Seminara G. 2009. A nonlinear model for river meandering. *Water Resour. Res.* 45:W04432

Callander RA. 1969. Instability and river channels. *J. Fluid Mech.* 36:465–80

Camporeale C, Perona P, Porporato A, Ridolfi L. 2005. On the long-term behavior of meandering rivers. *Water Resour. Res.* 41:W12403

Coleman E, Fenton JD. 2000. Potential-flow instability theory and alluvial stream bed forms. *J. Fluid Mech.* 418:101–17

Coleman E, Melville BW. 1994. Bed-form development. *J. Hydraul. Eng.* 120:544–60

Coleman SE, Melville BW. 1996. Initiation of bed forms on a flat sand bed. *J. Hydraul. Eng.* 122:301–10

Colombini M. 1993. Turbulence-driven secondary flows and formation of sand ridges. *J. Fluid Mech.* 254:701–19

Annu. Rev. Fluid Mech. 2010.42:43-66. Downloaded from www.annualreviews.org
by University of California - Berkeley on 02/08/12. For personal use only.

Colombini M. 2004. Revisiting the linear theory of sand dune formation. *J. Fluid Mech.* 502:1–16

Colombini M, Parker G. 1995. Longitudinal streaks. *J. Fluid Mech.* 304:161–83

Colombini M, Seminara G, Tubino M. 1987. Finite-amplitude alternate bars. *J. Fluid Mech.* 181:213–32

Colombini M, Stocchino A. 2005. Coupling or decoupling bed and flow dynamics: fast and slow sediment waves at high Froude numbers. *Phys. Fluids* 17:036602

Colombini M, Stocchino A. 2008. Finite-amplitude river dunes. *J. Fluid Mech.* 611:283–306

Culling WEH. 1965. Theory of erosion on soil-covered slopes. *J. Geol.* 73:230–54

Darby SE, Alabyan AM, Van de Wiel M. 2002. Numerical simulation of bank erosion and channel migration in meandering rivers. *Water Resour. Res.* 38:1163

Dietrich WE, Smith JD. 1983. Influence of the point bar on flow through curved channels. *Water Resour. Res.* 19:1173–92

Drake TG, Shreve RL, Dietrich WE, Whiting PJ, Leopold LB. 1988. Bedload transport of fine gravel observed by motion-picture photography. *J. Fluid Mech.* 192:193–217

Engelund F. 1970. Instability of erodible beds. *J. Fluid Mech.* 42:225–44

Engelund F, Fredsøe J. 1982. Sediment ripples and dunes. *Annu. Rev. Fluid Mech.* 14:13–37

Exner FM. 1925. Uber die wechselwirkung zwischen wasser und geschiebe in ussen. Sitzungber. *Acad. Wiss. Wien Math. Nat.* 134:165–80

Federici B, Seminara G. 2003. On the convective nature of bar instability. *J. Fluid Mech.* 487:125–45

Federici B, Seminara G. 2006. Effect of suspended load on bar instability. *Water Resour. Res.* 42:W07407

Frascati A, Lanzoni S. 2009. Morphodynamic regime and long-term evolution of meandering rivers. *J. Geophys. Res.* 114:F02002

Fredsøe J. 1974. On the development of dunes in erodible channels. *J. Fluid Mech.* 64:1–16

Fujita Y, Muramoto Y. 1985. Study on the process of development of alternate bars. *Bull. Disast. Prev. Res. Inst. Kyoto Univ.* 35(3):55–86

Garcia M, ed. 2008. *Sedimentation Engineering: Processes, Measurements, Modeling, and Practice*. ASCE Manuals Rep. Eng. Pract. 110. Reston, VA: ASCE

Giri S, Shimizu Y. 2006. Numerical computation of sand dune migration with free surface flow. *Water Resour. Res.* 42:W10422

Gunter A. 1971. Die kritische mittlere Sohlenschubspannung bei Geschiebemischungen unter Beriicksichtigung der Deckschichtbildung und der turbulenzbedingten Sohlenschubspannungsschwankungen. *Mitt. No. 3 Vers. Wasserbau, ETH Zurich*

Guy HP, Simons DB, Richardson EV. 1966. Summary of alluvial channel data from flume experiments 1956–61. *Geol. Survey Prof. Pap.* 462:I1–96

Howard AD. 1994. A detachment-limited model of drainage basin evolution. *Water Resour. Res.* 30:2261–86

Ikeda S, Parker G, Sawai K. 1981. Bend theory of river meanders. Part 1. Linear development. *J. Fluid Mech.* 112:363–77

Kennedy JF. 1963. The mechanism of dunes and antidunes in erodible-bed channels. *J. Fluid Mech.* 16:521–44

Lanzoni S, Siviglia A, Frascati A, Seminara G. 2006. Long waves in erodible channels and morphodynamic influence. *Water Resour. Res.* 42:W06D17

Lyn DA, Altinakar M. 2002. St. Venant-Exner equations for nearcritical and transcritical flows. *J. Hydraul. Eng.* 128:579–87

Lysne DK. 1969. Movement of sand in tunnels. *J. Hydraul. Div. Am. Soc. Civil Eng.* 95:1835–46

McLean SR, Smith JD. 1986. A model for flow over two-dimensional bed forms. *J. Hydraul. Eng.* 112:300–17

Nakagawa H, Tsujimoto T. 1980. Sand bed instability due to bedload motion. *J. Hydraul. Div. Am. Soc. Civ. Eng.* 106:2029–51

Olesen KW. 1983. Alternate bars and meandering of alluvial rivers. *Commun. Hydraul. Rep. 7-83*, Delft Univ. Technol., Delft, Netherlands

Parker G. 1984. Lateral bed load transport on side slopes. *J. Hydraul. Eng. ASCE* 110(HY2):197–99

Parker G, Paola C, Whipple KX, Mohrig D. 1998. Alluvial fans formed by channelized fluvial and sheet flow: theory. *J. Hydraul. Eng.* 124:1–11

Parker G, Sequeiros O. 2006. Large scale river morphodynamics: application to the Mississippi delta. *Proc. River Flow 2006 Conf. Lisbon*, ed. RML Ferreria, ECTL Avles, JGAB Leal, AH Cardoso, pp. 3–11. London: Taylor & Francis

Perron JT, Dietrich WE, Kirchner JW. 2008. Controls on the spacing of first-order valleys. *J. Geophys. Res.* 113:F04016

Richards KJ. 1980. The formation of ripples and dunes on an erodible bed. *J. Fluid Mech.* 99:597–618

Schielen R, Doelman A, de Swart HE. 1993. On the nonlinear dynamics of free bars in straight channels. *J. Fluid Mech.* 252:325–56

Schmeeckle MW, Nelson JM. 2003. Direct numerical solution of bedload transport using local, dynamic boundary condition. *Sedimentology* 50:279–301

Seminara G. 2006. Meanders. *J. Fluid Mech.* 554:271–97

Seminara G, Tubino M. 1992. Weakly nonlinear theory of regular meanders. *J. Fluid Mech.* 244:257–88

Seminara G, Zolezzi G, Tubino M, Zardi D. 2001. Downstream and upstream influence in river meandering. Part 2. Planimetric development. *J. Fluid Mech.* 438:213–30

Shields A. 1936. Anwendung der Ahnlichkeitsmechanik und der turbulenzforschung auf die geschiebebewegung. *Mitt. 26 Preuss. Vers. Wasserbau Schiffbau*

Sinha S, Parker G. 1996. Causes of concavity in longitudinal profiles of rivers. *Water Resour. Res.* 32:1417–28

Siviglia A, Nobile G, Colombini M. 2008. Quasi-conservative formulation of the one-dimensional Saint-Venant-Exner. *J. Hydraul. Eng.* 134:1521–26

Smith JD. 1970. Stability of a sand bed subjected to a shear flow at low Froude number. *J. Geophys. Res.* 75:5928–40

Smith TR, Bretherton FP. 1972. Stability and the conservation of mass in drainage basin evolution. *Water Resour. Res.* 8:1506–29

Swenson JB, Voller VR, Paola C, Parker G, Marr J. 2000. Fluvio-deltaic sedimentation: a generalized Stefan problem. *Eur. J. Appl. Math.* 11:433–52

Tubino M, Repetto R, Zolezzi G. 1999. Free bars in rivers. *J. Hydraul. Res.* 37:759–75

Venditti JG, Church M, Bennett SJ. 2005a. Morphodynamics of small-scale superimposed sand waves over migrating dune bed forms. *Water Resour. Res.* 41:W10423

Venditti JG, Church M, Bennett SJ. 2005b. On the transition between 2D and 3D dunes. *Sedimentology* 52:1343–59

Zolezzi G, Guala M, Seminara G, Termini D. 2005. Experimental observations of upstream overdeepening. *J. Fluid Mech.* 531:191–219

Zolezzi G, Seminara G. 2001. Downstream and upstream influence in river meandering. Part 1. General theory and application to overdeepening. *J. Fluid Mech.* 438:183–211

RELATED RESOURCES

Blondeaux P. 2001. Mechanics of coastal forms. *Annu. Rev. Fluid Mech.* 33:339–70

de Swart HE, Zimmerman JTF. 2009. Morphodynamics of tidal inlet systems. *Annu. Rev. Fluid Mech.* 41:203–29

Ikeda S, Parker G, eds. 1989. *River Meandering*. Water Resour. Monogr. 12. Washington D.C.: Am. Geophys. Union

Parker G. 2004. *1D Sediment Transport Morphodynamics with Applications to Rivers and Turbidity Currents*. **http://cee.uiuc.edu/people/parkerg/morphodynamics_ebook.htm.**

Annu. Rev. Fluid Mech. 2010.42:43-66. Downloaded from www.annualreviews.org
by University of California - Berkeley on 02/08/12. For personal use only.

Annual Review of
Fluid Mechanics

Volume 42, 2010

Contents

Annu. Rev. Fluid Mech. 2010.42:43-66. Downloaded from www.annualreviews.org
by University of California - Berkeley on 02/08/12. For personal use only.

Annu. Rev. Fluid Mech. 2010.42:43-66. Downloaded from www.annualreviews.org
by University of California - Berkeley on 02/08/12. For personal use only.

Indexes

Errata

An online log of corrections to *Annual Review of Fluid Mechanics* articles may be found at http://fluid.annualreviews.org/errata.shtml